Coherence Switching in a Four-Level System: Quantum Switching

Byoung S. Ham
Telecommunications Basic Research Laboratory, Electronics and Telecommunications Research Institute, Daejun, 305-350 Korea

Philip R. Hemmer
U.S. Air Force Research Laboratory, Hanscom Air Force Base, Massachusetts 01731
(Received 25 October 1999)

Dark resonance switching among three-laser interactions in a four-level system is observed by using an enhanced nondegenerate four-wave mixing technique. This coherence switching mechanism is based on simultaneous suppression and enhancement of two-photon absorption and has a novel application to high-speed optical switches.

PACS numbers: 42.50.Gy, 42.65.Pc, 42.70.Mp, 78.20.Bh

In this Letter, we have observed simultaneous enhancement and suppression of the dark resonance [1–3] for the first time by use of the nondegenerate four-wave mixing technique. This demonstration shows potential applications of quantum interference phenomena to ultrahigh-speed (all) optical switches such as in fiber-optic communications. The energy level structure used for this observation is composed of three-hyperfine states (ground states) and an excited state, which is common in rare-earth doped solids. Unlike atomic systems, spectral hole burning solids have some practical advantages of robustness, compactness, nonatomic diffusion, and spectral selectivity. Very recently enhancement of the four-wave mixing signal was demonstrated in a persistent spectral hole-burning solid [4]. Moreover, several demonstrations of electromagnetically induced transparency (EIT) [3] based nonlinear optical processes in solids such as optical memories [5], enhanced phase conjugation [6], and rf-field coupled optical gain [7], open the door to practical applications of the dark resonance.

In a three-level Λ-type system Raman laser fields (Ω_1 and Ω_2) induce superposition states, which are decoupled ($|-\rangle$) and coupled ($|+\rangle$) from the excited state ($|\varepsilon\rangle$):

$$|-\rangle = (\Omega_2|\alpha\rangle - \Omega_1|\beta\rangle)/\Omega\,, \qquad (1)$$

$$|+\rangle = (\Omega_1|\alpha\rangle + \Omega_2|\beta\rangle)/\Omega\,, \qquad (2)$$

where $\Omega^2 = \Omega_1^2 + \Omega_2^2$ [see Fig. 1(a)]. The essential feature of the decoupled state is coherent population trapping (CPT) [1] or dark resonance. The existence of the dark resonance is a basis of nonabsorption resonances [1,2], EIT, and many potential applications of nonlinear optical processes, such as resonant enhancement of refractive index [8], lasers without inversion [9], up-conversion lasers [10], and high-resolution spectroscopy [11]. In general, CPT can create large spin coherence (dark resonance) capable of producing EIT in an optically dense medium. CPT, however, is not adequate for any application that needs coherence buildup faster than the excited-state lifetime. This is because CPT is inherently based on the optical pumping mechanism.

Recently, Ham *et al.* proposed efficient spin coherence excitation in an atom-shelving system [12]. The spin

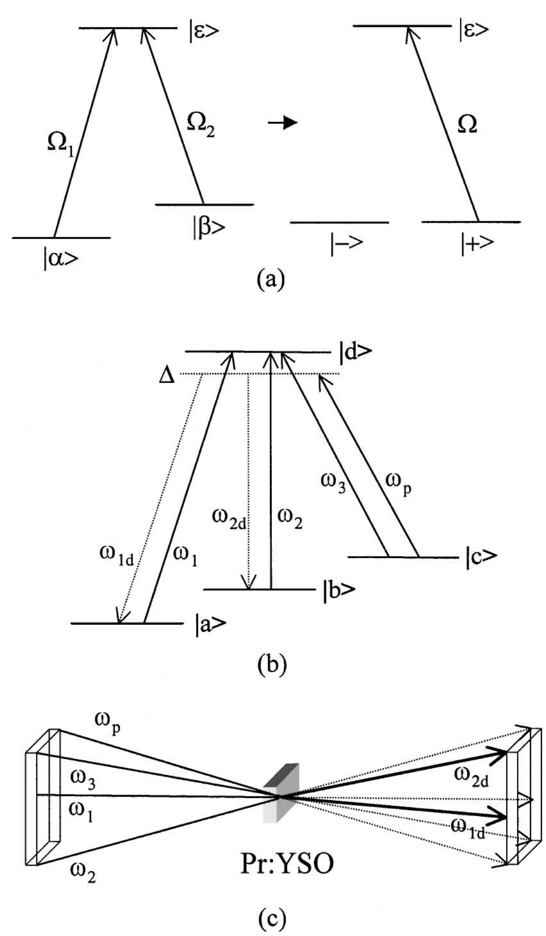

FIG. 1. (a) Resonant Raman interactions with a three-level system in bare-state basis and coherent-state basis. (b) Energy schematic for coherence switching in a four-level system: dephasing rates among $|a\rangle$, $|b\rangle$, and $|c\rangle$ are negligible. (c) Beam propagation geometry for (b).

0031-9007/00/84(18)/4080(4)$15.00

coherence excitation by the optical Raman fields in that system can be faster than the excited-state lifetime. The efficiency of the dark resonance in that system is also higher than that in quantum beat [13] or coherent Raman beat [14]. Especially, the dark-resonance excitation can be as fast as the inverse of the applied Rabi frequency [12]. Therefore, in an extreme case of zero excited-state lifetime, the pumped atoms should oscillate between the excited state $|\varepsilon\rangle$ and the coupled state $|+\rangle$. The Raman-field excited spin coherence $\rho_{\alpha\beta}$ also oscillates as fast as the Rabi flopping (between $|+\rangle$ and $|\varepsilon\rangle$) occurs.

In a four-level optical system, however, such dark resonance can be perturbed by a third laser field. In this case, the third laser field can control the nonlinear optical properties induced by the Raman fields. Therefore, the two-photon absorption of the Raman fields can be either enhanced or suppressed. This type of coherence control was proposed by Agarwal *et al.* using a cascade four-level system [15]. Hemmer *et al.* demonstrated the enhancement of optical nonlinearity owing to CPT in a double-Λ four-level system [16]. Imamoglu *et al.* also demonstrated giant Kerr nonlinearity owing to EIT [17]. Not only nonlinearity, but also linearity should be changed in such a system. Harris *et al.* proposed photon switches by using two-photon linearity control [18].

Figure 1(b) shows a partial energy level diagram of 0.05 at.% rare-earth Pr^{3+} doped Y_2SiO_5 (Pr:YSO). For this work, the relevant optical transition is ${}^3H_4 \rightarrow {}^1D_2$, and the resonance frequency is 606 nm [19]. The measured absorption coefficient α for that transition is $\sim$10 cm^{-1}. The inhomogeneous width of the optical transitions is $\sim$4 GHz at liquid helium temperatures, which is much wider than the hyperfine splitting. The observed optical homogeneous width of Pr:YSO is temperature dependent, which is exponentially broadened as temperature increases in the range of 4 to 6 K, while the spin homogeneous width is almost constant [5]. Ground (${}^3H_4$) and excited (${}^1D_2$) states each have three doubly degenerate hyperfine states and, due to the low-symmetry crystal field, the wave functions are mixed, causing the selection rule to break down for electronic dipole transitions between electronic singlets [19]. The energy splittings between the hyperfine states of the ground level ${}^3H_4$ are 10.2 MHz for $|c\rangle \leftrightarrow |b\rangle$, 17.3 MHz for $|b\rangle \leftrightarrow |a\rangle$, and 27.5 MHz for $|c\rangle \leftrightarrow |a\rangle$ [20]. The ground state population decay time T_1^s is $\sim$100 s, and spin transverse decay time T_2^s for the 10.2-MHz transition is 500 μs at 6 K [5]. Because of the long population decay time on the hyperfine states of the ground level, optical hole burning persists until the populations are redistributed among the three-hyperfine states.

In Fig. 1(b), the Raman laser fields ω_1 and ω_2, ω_1 and ω_3, and ω_2 and ω_3 each can induce phase grating on the hyperfine states. Here it should be noted that the Rabi frequency does not need to be strong enough ($\Omega \gg \gamma$) to reach near maximal coherence, because the Raman coherence amplitude depends on the pulse area Θ: $\Theta = \int_0^t \Omega(t')\,dt'$. However, in an optically thick medium a strong Rabi frequency has an advantage of generating strong four-wave mixing signals due to high EIT efficiency. For the resonant Raman transition, the difference frequency among ω_1, ω_2, and ω_3 should match the hyperfine splitting, and each optical frequency should be resonant with its transition. Laser field ω_p acts as a probe (read) beam, which scatters off the two-photon coherence phase gratings and generates the four-wave mixing signals ω_{1d} and ω_{2d} satisfying phase matching conditions $\mathbf{k}_{1d} = \mathbf{k}_1 - \mathbf{k}_3 + \mathbf{k}_p$ and $\mathbf{k}_{2d} = \mathbf{k}_2 - \mathbf{k}_3 + \mathbf{k}_p$, respectively [see Fig. 1(c)]. In Fig. 1(c) noncollinear propagation scheme has an advantage of background-free detection of the four-wave mixing signals [4].

A stabilized cw ring dye laser output is split into four-laser beams ω_1, ω_2, ω_3, and ω_p by acousto-optic modulators driven by frequency synthesizers (PTS 160). Although the ring dye laser jitter is $\sim$1–2 MHz, the difference frequencies among the four-laser beams are always kept less than kHz. All the laser beams are focused into the sample by a 30-cm-focal-length lens. The focused beam diameter (e^{-1} in intensity) is $\sim$100 μm. The power of the lasers ω_1, ω_2, ω_3, and ω_p are 12, 25, 10, and 21 mW, respectively. The angle between the beams is about $\sim$80 mrad. The persistent spectral hole-burning crystal of Pr:YSO is inside a cryostat and the temperature is kept at 6 K. The size of the crystal is 3.5 mm $\times$ 4 mm $\times$ 3 mm, and optical B-axis is along the 3-mm length. The laser propagation direction is almost parallel to the optical axis.

Figures 2(a) and 2(b) show experimental data of the four-wave mixing signals $I_{2d}(\omega_2)$ and $I_{1d}(\omega_1)$ as a function of δ_1 in a three-laser acting four-level system, respectively. Here we define $\delta_1 = \omega_{ad} - \omega_1$. The laser beam ω_2 is blueshifted from the resonance frequency, i.e., $\delta_2 = \omega_{bd} - \omega_2 = -10$ kHz. This intentional detuning of δ_2 is to show an asymmetric feature of the dark resonance, where $|\delta_2|$ is less than the spin inhomogeneous width (29 kHz) for the 10.2-MHz transition or the Rabi frequency. The overall spectral width of $I_{2d}(\omega_{2d})$ in Fig. 2(a) is $\sim$1 MHz. Obviously, the four-wave mixing generation exists if the detuning δ_1 is within the modified optical inhomogeneous width, and the Raman difference frequency δ_2 is less than the spin inhomogeneous width. As mentioned above the optical inhomogeneous width in this system is modified by the laser jitter due to the persistent spectral hole burning. Therefore, the overall spectral width of $I_{2d}(\omega_{2d})$ also demonstrates the modified optical inhomogeneous width, and the ω_1 acts as a repump within the laser jitter if $|\delta_1|$ is not less than the spin inhomogeneous width (or the applied Rabi frequency).

In Fig. 2 the signal intensity $I_{2d}(\omega_{2d})$ becomes substantially suppressed as the detuning δ_1 comes close to zero, while the signal intensity $I_{1d}(\omega_{1d})$ is greatly enhanced. This signal enhancement of $I_{1d}(\omega_{1d})$ and the suppression of $I_{2d}(\omega_{2d})$ at $\delta_1 = 0$ are due to the dark resonance changes in the hyperfine states $|a\rangle - |c\rangle$ and

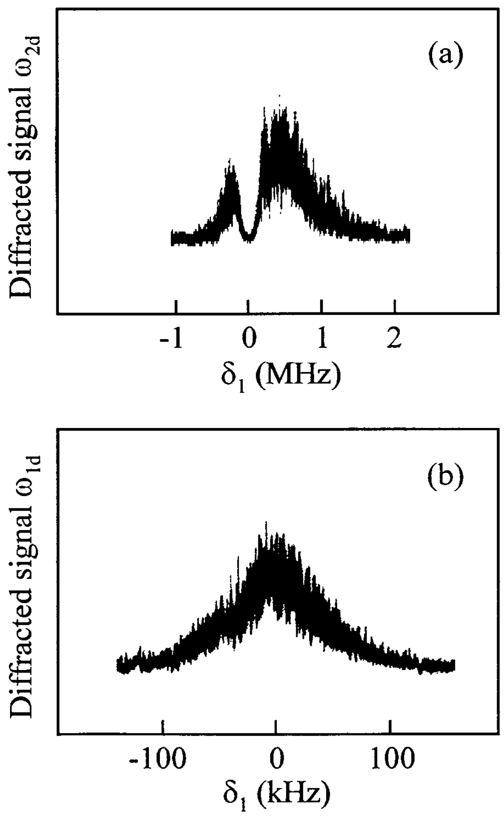

FIG. 2. Intensity of the four-wave mixing signals (a) $I_{2d}(\omega_{2d})$ and (b) $I_{1d}(\omega_{1d})$; $\delta_1 = \omega_{ad} - \omega_1$, $\omega_2 = \omega_{bd} + 10$ kHz, $\omega_3 = \omega_{cd}$, and $\Delta = 1.5$ MHz; $\omega_{ij} = \omega_j - \omega_i$.

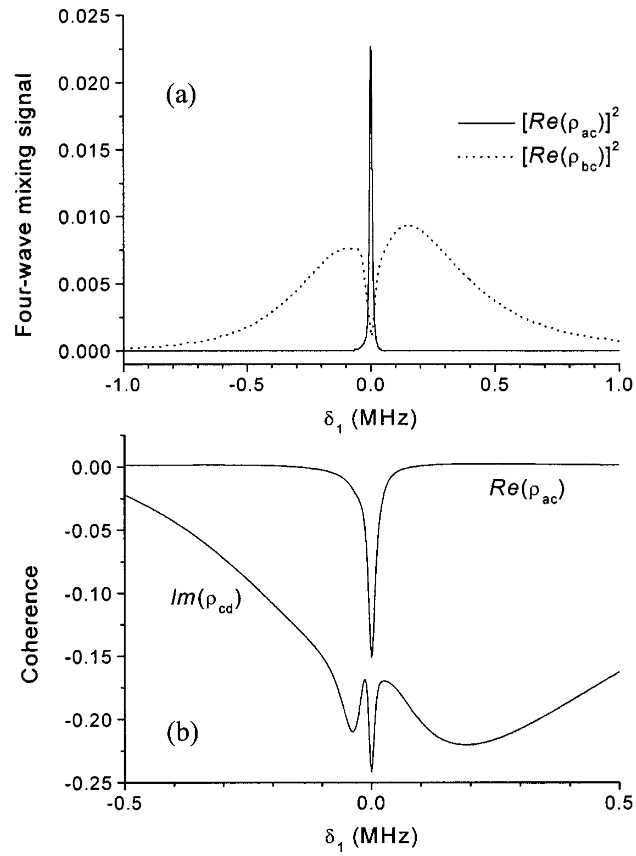

FIG. 3. Numerical calculations of three-laser interactions with a four-level system for (a) spin-coherence intensity and (b) optical-coherence reduction vs spin-coherence enhancement as a function of δ_1; $\Omega_1 = 40$, $\Omega_2 = 100$, $\Omega_3 = 60$ kHz, $\gamma_{da} = \gamma_{db} = \gamma_{dc} = 100$ kHz, $\Gamma_{da} = \Gamma_{db} = \Gamma_{dc} = 6$ kHz, $\gamma_{ba} = \gamma_{ca} = \gamma_{cb} = 1$ kHz, and $\Gamma_{ba} = \Gamma_{ca} = \Gamma_{cb} = 0$.

$|b\rangle - |c\rangle$, respectively. The suppressed spectral width of $I_{2d}(\omega_{2d})$ at $\delta_1 = 0$ in Fig. 2(a) is narrower than the laser jitter, and it is an experimental proof that the four-wave mixing generation is based on the dark resonance. Here it should be noted that the intensity of the nondegenerate four-wave mixing signals depends on the probe detuning Δ and exists only if all three lasers interact with the system (due to the persistent spectral hole burning) [4]. For cw lasers, unlike time-delayed pulsed lasers [6], Δ should not be zero; otherwise, degenerate four-wave mixing (population grating) phenomena dominate it: This will be discussed in more detail in a separate paper. As demonstrated already in Ref. [6], the intensity of the dark-resonance based nondegenerate four-wave mixing signal is proportional to the Raman induced coherence strength in the hyperfine states. Therefore, the swap of the diffraction signals' intensity at $\delta_1 = 0$ in Fig. 2 is due to the perturbation of the Raman dark states when all three beams are resonant to the system. The enhanced diffraction signal $I_{1d}(\omega_{1d})$ in Fig. 2(b) is owing to one-photon absorption reduction (increased dark-resonance efficiency) in the transition $|a\rangle - |d\rangle$: This will be discussed in Fig. 3.

To analyze the experimental results in Fig. 2, we did numerical calculations by solving 16 density matrix equations for Fig. 1(b). In Fig. 1(b), the Hamiltonian in an interacting picture is

$$H = h/2\pi\{-\delta_1|a\rangle\langle a| - \delta_2|b\rangle\langle b| - \delta_3|c\rangle\langle c| - \tfrac{1}{2}(\Omega_1|a\rangle\langle d| + \Omega_2|b\rangle\langle d| + \Omega_3|c\rangle\langle d|) + \text{H.c.}\}, \tag{3}$$

where $\delta_1 = \omega_{ad} - \omega_1$, $\delta_2 = \omega_{bd} - \omega_2$, $\delta_3 = \omega_{cd} - \omega_3$, h is Plank's constant, and Ω_i is Rabi frequency of the laser beam ω_i ($i = 1, 2, 3$). The time-dependent density-matrix equation of motion is

$$\frac{\partial\rho}{\partial t} = -\frac{i}{\hbar}[H,\rho] - \tfrac{1}{2}\{\Gamma,\rho\}, \tag{4}$$

where $\{\Gamma,\rho\} = \Gamma\rho + \rho\Gamma$ [21]. Figure 3 shows the results of the numerical calculations. For these calculations a closed four-level system is assumed, and experimental values are used for the parameters. The optical homogeneous width is replaced by the laser jitter for simplicity, because the optical inhomogeneous modification is limited by the laser jitter in this experiment. The spin inhomogeneous broadening of 30 kHz is considered. In Fig. 3(a), the spin coherences $\mathrm{Re}(\rho_{ac})$ and $\mathrm{Re}(\rho_{bc})$ are calculated as a function of detuning δ_1, when $\delta_2 = -10$ kHz and $\delta_3 = 0$.

As seen in Fig. 3(a), the laser beams ω_2 and ω_3 induce spin coherence $\mathrm{Re}(\rho_{bc})$ on the hyperfine transition $|b\rangle - |c\rangle$, so that the probe ω_p scatters off the coherence phase grating $[\mathrm{Re}(\rho_{bc})]^2$ and generates a four-wave mixing signal $I_{2d}(\omega_2)$. The four-wave mixing signal intensity is proportional to the square of the Raman field excited spin coherence directly [6]:

$$I_{2d(1d)}(\omega_{2d(1d)}) \propto [\mathrm{Re}(\rho_{bc(ac)})]^2 I_p(\omega_p)\,. \qquad (5)$$

When the field ω_1 comes close to the resonance ($\delta_1 = 0$), however, the phase grating $[\mathrm{Re}(\rho_{bc})]^2$ becomes suppressed, while $[\mathrm{Re}(\rho_{ac})]^2$ is greatly enhanced. Therefore, ω_2 seems to act as a control field enhancing the dark resonance on the hyperfine transition $|a\rangle - |c\rangle$ and suppressing that on the transition $|b\rangle - |c\rangle$. The numerical calculations in Fig. 3(a) match the experimental data in Fig. 2.

In Fig. 3(b), the spin coherence $\mathrm{Re}(\rho_{ac})$ is compared with the absorption spectrum of the beam ω_3, $\mathrm{Im}(\rho_{cd})$. As seen, the coherence enhancement in $\mathrm{Re}(\rho_{ac})$ is caused by the absorption increase (or coherence decrease) in $\mathrm{Im}(\rho_{cd})$, which leads to coherence decrease in $\mathrm{Re}(\rho_{bc})$. This absorption increase of the beam ω_3 is due to decoherence in the dark state caused by the interaction of the beam ω_1. Note that the spectral linewidth of the absorption recovery in $\mathrm{Im}(\rho_{cd})$ at $\delta_1 = 0$ is similar to that of the enhanced coherence spectral width of $\mathrm{Re}(\rho_{ac})$. The asymmetric feature of the coherence curves in Fig. 3 is due to the detuning of δ_2. As demonstrated previously in an atom-shelving system, the two-photon coherence can be as fast as the applied Rabi frequency [5,6,12]. So does the quantum switching time. This is because most rare-earth doped solids have slower optical decay time ($\sim$ms), and, thus, the coherence excitation is dominated by the population difference between the $|+\rangle$ state and the excited state $|\varepsilon\rangle$ as mentioned in Fig. 1(a).

In conclusion, a novel experiment of coherence switching has been demonstrated for the first time in a four-level (solid) system. Even though the observed extinct ratio of the coherence switching in Fig. 3 shows potential applications to low-threshold, high-speed optical switches, temperature-dependent quantum interference in rare-earth doped solids still remains as a problem to overcome [22]. For the implementation of (all) optical quantum switches in fiber-optic communications, therefore, semiconductors having quantum-well structures should be studied because the optical oscillator strengths are big and the communication wavelength can be used directly. Very recently, EIT has been observed in an InGaAs multiple quantum-well semiconductor [23].

The author (B. S. H.) thanks Telecommunications Basic Research Laboratory, ETRI for financial support. The experiment was done in the U.S. AFRL, Hanscom AFB, MA.

[1] H. R. Gray, R. M. Whitley, and C. R. Stroud, Jr., Opt. Lett. **3**, 218 (1978).
[2] G. Alzetta, A. Gozzini, L. Moi, and G. Orrilos, Nuovo Cimento Soc. Ital. Fis. **36B**, 5 (1976).
[3] S. E. Harris, Phys. Today **50**, No. 7, 36 (1997), and references therein.
[4] B. S. Ham, M. S. Shahriar, and P. R. Hemmer, Opt. Lett. **22**, 1138 (1997); **24**, 86 (1999).
[5] B. S. Ham, M. S. Shahriar, M. K. Kim, and P. R. Hemmer, Opt. Lett. **22**, 1849 (1997).
[6] B. S. Ham, P. R. Hemmer, and M. S. Shahriar, Phys. Rev. A **59**, R2583 (1999). For $I_d \propto I_p$ in Eq. (5), refer to B. Lu *et al.*, Opt. Lett. **23**, 804 (1998).
[7] B. S. Ham, M. S. Shahriar, and P. R. Hemmer, J. Opt. Soc. Am. B **15**, 1541 (1998).
[8] L. V. Hau, S. E. Harris, Z. Dutton, and C. H. Behroozi, Nature (London) **397**, 594 (1999); M. O. Scully, Phys. Rev. Lett. **67**, 1855 (1991).
[9] A. S. Zibriv, M. D. Lukin, D. E. Nikonov, L. Hollberg, M. O. Scully, V. L. Velichansky, and H. O. Robinson, Phys. Rev. Lett. **75**, 1499 (1995).
[10] S. E. Harris, J. E. Field, and A. Imamoglu, Phys. Rev. Lett. **64**, 1107 (1990); M. Jain, H. Xia, G. Y. Yin, A. J. Merriam, and S. E. Harris, Phys. Rev. Lett. **77**, 4326 (1996).
[11] M. D. Lukin, M. Fleischhauer, A. S. Zibriv, H. G. Robinson, V. L. Velichansky, L. Hollberg, and M. O. Scully, Phys. Rev. Lett. **79**, 2959 (1997).
[12] B. S. Ham, M. S. Shahriar, M. K. Kim, and P. R. Hemmer, Phys. Rev. B **58**, R11 825 (1998).
[13] R. M. Shelby, A. C. Tropper, R. T. Harley, and R. M. Macfarlane, Opt. Lett. **8**, 304 (1983); Y. Fukuda, M. Tanigawa, and T. Hashi, *ibid.* **8**, 301 (1983).
[14] T. Blasberg and D. Suter, Phys. Rev. B **51**, 6309 (1995).
[15] G. S. Agarwal and W. Harshawardhan, Phys. Rev. Lett. **77**, 1039 (1996).
[16] P. R. Hemmer, D. P. Katz, J. Donoghue, M. Cronin-Golomb, M. S. Shahriar, and P. Kumar, Opt. Lett. **20**, 982 (1995).
[17] A. Imamoglu, H. Schmidt, G. Woods, and M. Deutsch, Phys. Rev. Lett. **79**, 1467 (1997).
[18] S. E. Harris and Y. Yamamoto, Phys. Rev. Lett. **81**, 3611 (1998).
[19] K. Holliday, M. Croci, E. Vauthey, and U. P. Wild, Phys. Rev. B **47**, 14 741 (1993).
[20] R. W. Equall, R. L. Cone, and R. M. Macfarlane, Phys. Rev. B **52**, 3963 (1995).
[21] M. O. Scully and M. S. Zubairy, *Quantum Optics* (Cambridge University Press, Cambridge, England, 1997).
[22] For the EIT efficiency versus optical decay rate γ, see Y.-Q. Li and M. Xiao, Phys. Rev. A **51**, 4959 (1995) for atomic vapors. In rare-earth doped solids, $\gamma \propto \exp(T)$; see Ref. [5] and B. S. Ham *et al.*, J. Opt. Soc. Am. B **16**, 803 (1999), and references therein.
[23] G. B. Serapiglia, E. Paspalakis, C. Sirtori, K. L. Vodopyanov, and C. C. Philips, Phys. Rev. Lett. **84**, 1019 (2000). For more information, see H. Schmidt *et al.*, Laser Phys. **9**, 797 (1999).